Journal of Computer Science

Research Article

An Adaptive Detail Preserving Modified Progressive Pca Thresholding Based Image Denoising

N. Anilkumar[1], S. Radhakrishnan[2], Shaik Syed Basha[2], Hari Krishna Deevi[2] and Md. Umar Khan[3]

[1]*Department of CSE, G. Narayanamma Institute of Technology and Science, Hyderabad, India*
[2]*Department of CSE (AI and ML), KKR and KSR Institute of Technology and Sciences, Guntur, India*
[3]*Department of CSE, Kallam Haranatha Reddy Institute of Technology, Chowdavaram, Guntur, India*

Article history
Received: 05-08-2025
Revised: 16-07-2026
Accepted: 05-06-2026

Corresponding Author:
S. Radhakrishnan
Department of CSE (AI and ML), KKR and KSR Institute of Technology and Sciences, Guntur, India
Email: radki1970@gmail.com

Abstract: Radiologists use medical imaging tools to assess the anatomy and function of interior organs. However, medical images are frequently distorted by various types of noise generated during the capture, transmission, and reconstruction operations, which can dramatically reduce image quality and hide critical diagnostic features. As a result, developing effective denoising algorithms that suppress noise while maintaining structural information remains a significant challenge in medical image processing. To address this issue, this work presents an adaptive cluster-wise progressive denoising algorithm for maintaining detail in medical images. The suggested method groups similar picture patches using adaptive clustering and then uses progressive Principal Component Analysis (PCA) thresholding guided by the Marchenko-Pastur (MP) law to eliminate noise while retaining significant image information. The denoising technique is further improved by employing a low-rank matrix representation to maintain the image's structural properties. The proposed approach is effective, as demonstrated by experimental results acquired using MATLAB on medical images damaged with Gaussian noise at various noise levels. The method's performance is measured using statistical metrics such as Peak Signal-To-Noise Ratio (PSNR), Mean Squared Error (MSE), and Contrast to Noise Ratio (CNR). The findings show that the suggested method outperforms existing denoising methods in terms of noise suppression while conserving critical anatomical characteristics.

Keywords: Principal Component Analysis, Marchenko Pastur (MP) Law, Image Denoising

Introduction

In sectors such as medicine, space exploration, radar, and machine vision, among others, images are considered potential sources of information. Image processing is therefore thought to be the most difficult task in these domains. The performance of image processing techniques is made possible by the rapid advancement of computer technology, which enhances the quality of images generated by a variety of instruments, including scanners, cameras, machine vision systems, and ultrasounds. During image acquisition, storage, and transmission, noise affects these images, which is not what is wanted in clinical image processing. The intensity of pixels in an image will change due to noise. Gaussian noise is the term used to describe noise produced by digital equipment as a result of electrical disruptions. Medical images are also impacted by other noises, such as gamma, exponential, speckle, uniform, salt and pepper, Rayleigh, and photon noise. Many researchers have applied different denoising algorithms in different domains, such as the filtering domain (Baselice et al., 2018; Ali, 2018; You and Kaveh, 2000; Buades et al., 2005) transform domain (Agrawal and Sahu, 2012; Starck et al., 2002; Jannath et al., 2016), machine learning domain (Gondara, 2016; Ackley et al., 1988; Jain et al., 2009; Misra et al., 2013; Pour and Javanshir, 2017), and statistical domain (Rajan et al., 2011; Luo et al., 2010; Awate and Whitaker, 2005; Sudeep et al., 2015; He and Greenshields, 2009), taking into consideration different statistical parameters like PSNR, CNR, etc., to diminish the noise effect in medical images.

Medical imaging modalities such as MRI, CT, ultrasound, and X-ray imaging are critical in current clinical diagnosis and treatment planning. However, these imaging systems are frequently hampered by numerous types of noise during the acquisition and reconstruction stages. For example, MRI images are frequently distorted by Gaussian and Rician noise, whereas CT images may be affected by photon and electronic noise. These distortions can impair image quality and hide crucial anatomical structures; therefore, dependable denoising procedures are required for accurate medical interpretation. As a result, developing effective denoising algorithms that can preserve structural information while suppressing noise is an essential research topic in medical image processing.

Recently, various cutting-edge image denoising techniques have been presented, utilizing transform-domain and deep learning frameworks. Wavelet-based denoising approaches use sparse image representations in the wavelet domain and thresholding procedures to reduce noise while keeping structure. Similarly, curvelet and contourlet transforms have proven to be more effective at capturing directional features and fine textures in medical images. In recent years, deep learning-based models such as Convolutional Neural Networks (CNNs) and autoencoder architectures have been frequently used for image denoising. These algorithms develop complicated mappings between noisy and clean images from big datasets, resulting in higher denoising performance. They do, however, demand a large amount of training data and processing power. As a result, lightweight statistical and matrix-based techniques, such as PCA-based denoising, continue to be desirable for medical imaging applications that require computing efficiency and interpretability.

As the Block Matching 3-Dimensional (BM3D) algorithm performs worse on images with high noise levels, a two-fold bounded BM3D technique has been introduced by Chen and Wu (2010); Lebrun (2012) has improved the BM3D algorithm's transparency by taking into account a new notation that operates in spatial dimensions in addition to the third dimension. To apply the BM3D technique to huge image patches, Burger et al. (2012) have linked it to a simple multi-layer perceptron, before using non-local similarity between grouped blocks and local sparsity of wavelet coefficients. Zhong et al. (2015) suggested a way to eliminate the one-dimensional transform between blocks and to introduce a non-local centralization.

The BM3D technique has been implemented on heterogeneous computer platforms by Sarjanoja et al. (2015) utilizing OpenCL and CUDA approaches to increase the computation speed at a pace of 7.5 times quicker than the original performance. In order to accomplish self-adaptation and shorten the implementation time, BM3D was used in combination with the Total Variation technique by Li et al. (2017). Hasan and El-Sakka (2018) boosted the BM3D performance by raising the Structural Similarity Index value rather than decreasing the Mean Squared Error value. A methodology for precise estimations of effective approximations and the noise-power spectrum has been introduced by Makinen et al. (2019). They have also assessed noise variances that are correlated in comparable blocks.

Although several denoising approaches have been presented in the literature, each one has drawbacks. Traditional filtering methods are computationally straightforward, but they frequently result in excessive smoothing, causing critical anatomical details to be lost in medical images. Transform-domain techniques, such as wavelet and curvelet-based algorithms, increase noise suppression by leveraging sparse representations; however, their performance is heavily reliant on the selection of proper transform coefficients and thresholding schemes. Advanced approaches, such as BM3D, provide good denoising performance by utilizing non-local similarities across image patches, although they are frequently computationally intensive and may struggle with images with significant noise changes. In recent years, deep learning-based denoising techniques have shown promise; nevertheless, these models often require large annotated datasets and significant computer resources to train. As a result, efficient denoising algorithms that can successfully reduce noise while conserving structural information are still required, even without considerable training data or processing resources. Motivated by these challenges, we propose an adaptive detail-preserving modified progressive PCA thresholding framework that combines adaptive clustering and statistically guided PCA thresholding to achieve efficient noise suppression while preserving important structural details in medical images.

Despite the fact that various medical picture denoising algorithms exist, many of them struggle to preserve fine structural details or are computationally complicated. Traditional filtering methods frequently obscure crucial anatomical features, but transform-domain and deep learning algorithms may necessitate extensive training datasets or sophisticated parameter tweaking. To address these limitations, this research suggests an adaptive detail-preserving modified progressive PCA thresholding paradigm for medical picture denoising.

The proposed approach is unusual in that it combines adaptive clustering, statistically guided PCA thresholding, and detail-preserving enhancement inside a unified denoising framework. Unlike traditional PCA-based techniques, the proposed method uses an adaptive clustering mechanism to group structurally related image patches, allowing for more efficient use of local image redundancy. Furthermore, the Marchenko Pastur (MP) law-based progressive PCA thresholding is employed to automatically select the best threshold levels for distinguishing noise from meaningful signal components. This method enhances noise suppression while preserving the structural integrity of medical images. Furthermore, a low-rank matrix representation is used to preserve crucial anatomical features during the denoising procedure.

Despite tremendous progress in image denoising, many existing algorithms still struggle to balance noise removal and detail preservation. Techniques like BM3D and deep learning models can achieve great denoising performance, but they are frequently computationally complex and require huge training datasets. As a result, there is a demand for efficient denoising frameworks that can efficiently suppress noise while keeping crucial structural information in medical images. To address this issue, this paper proposes an adaptive detail-preserving modified progressive PCA thresholding strategy that combines adaptive clustering and statistically guided PCA-based noise separation to increase denoising performance while remaining computationally efficient.

The key contributions of this work are summarized as follows:

- Created an adaptive clustering technique that automatically groups similar image patches based on structural properties
- Added Marchenko Pastur law-guided progressive PCA thresholding for better separation of noise and signal components
- Implemented a detail-preserving low-rank denoising approach to preserve significant anatomical structures in medical images
- Experimental validation on noisy medical images shows better performance in terms of PSNR, MSE, and CNR than previous denoising approaches

Preliminaries

The following steps make up the suggested method for medical image denoising that is provided in this research. Initially, a selected medical image from the database is subjected to Gaussian noise at different standard deviation levels (e.g., 10, 20, 30, 40, and 50). The suggested method, which is depicted in Figure 1, then finds the edges of the damaged images and denoises them, as will be discussed in the subsections that follow.

Adaptive Magnitude Gradient

The magnitude gradient (Xue et al., 2014) shows how each pixel's intensity varies in an image. The magnitude gradient is used to evaluate intensity discontinuities in the image. The use of Euclidean distance is this method's primary drawback. Numerous problems with Euclidean distance exist, including the reduction of sparsity, the curse of dimensionality, and non-scale invariance. An Adaptive Magnitude Gradient (AMG) approach is taken into consideration in the suggested solution in order to overcome these problems. This technique computes changes in the image's intensity with respect to the Hausdorff distance between each pixel in the x and y directions. A Hausdorff distance has fewer points taken into account than a Euclidean distance, which reduces computational complexity and boosts computational performance, as shown in Algorithm 1.

Algorithm 1

Source: Medical image
Output: The medical image's gradient magnitude
Step 1: Determine the size of the image by considering it.
Step 2: Let sigma have a value of 0.6 (σ).
Step 3: Using the formulas provided in Equations (4) and (5), compute the Gaussian (Gaus) and derivative of the Gaussian (Gaus_der):

$$Gaus(x;\mu,\sigma^2)=\frac{1}{\sqrt{(2\pi\sigma^2)}}e-\frac{(x-\mu^2)}{2\sigma^2} \tag{4}$$

$$Gaus\_der(x;\mu,\sigma^2)=\frac{d}{dx}(Gau(x;\mu,\sigma^2)) \tag{5}$$

Step 4: Determine the intensity on the horizontal axis using the values shown in equations (6) and (7).

$$temp\_h=I\otimes(1/Gaus) \tag{6}$$

$$horizontal=temp\_h\otimes Gaus\_der \tag{7}$$

Step 5: Determine the intensity along the vertical axis using the equations (8) and (9) that follow.

$$temp\_v=I\otimes Gaus \tag{8}$$

$$vertical=temp\_v\otimes Gaus\_der \tag{9}$$

Where the Gaussian and Gaussian derivatives are denoted by Gaus and Gaus_der.
Step 6: Determine the gradient angle and gradient magnitude by utilizing the inverse tangent of the medical image and the Hausdorff distance, respectively.

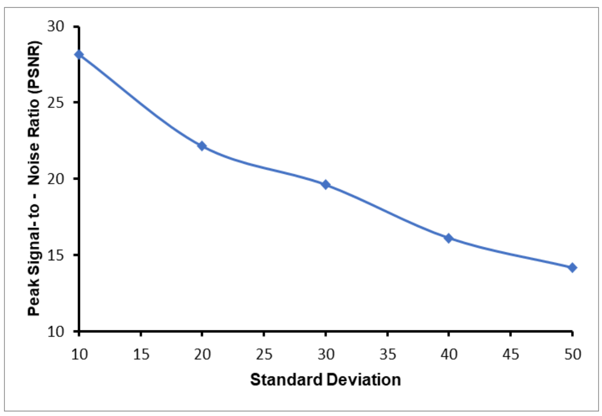

Fig. 1: Peak Signal- to - Noise Ratio (PSNR) MRI image at various Standard Deviations

Adaptive-Clustering

Adaptive clustering is a powerful technique for dynamically segmenting data, particularly in non-stationary environments. This paper presents a novel Adaptive Clustering Algorithm (ACA) that dynamically adjusts cluster centroids based on data distribution and density variations. The proposed method integrates density estimation, real-time centroid updates, and an adaptive thresholding mechanism. Experimental results demonstrate improved clustering accuracy, robustness, and computational efficiency compared to traditional clustering algorithms, as shown in Algorithm 2.

Algorithm 2

Step 1: Initialization: Randomly select initial cluster centers or use a density-based seeding method.
Step 2: Density Estimation: Calculate the local density of data points using a predefined density function.
In the proposed framework, edge detection is critical for maintaining structural features in the medical image. Medical images contain anatomical boundaries that are essential for diagnosis. Conventional denoising algorithms frequently distort the edges while reducing noise. As a result, an adaptive gradient-based edge detection approach is used to identify major structural boundaries before denoising. The identified edge information is used during the denoising stage to guarantee that noise reduction does not alter essential image features.
Step 3: Centroid Update: Adjust cluster centers based on the density distribution of the data.
Step 4: Adaptive Thresholding: Determine an adaptive threshold for merging or splitting clusters depending on the density variations in the dataset.
Step 5: Convergence Check: Stop the algorithm when the changes in cluster centers fall below a predefined threshold, indicating stability.

Automatic Cluster Count Determination and Adaptive Thresholding

The local patch density is calculated to capture structural similarities and texture redundancy in the image. Density-aware selection is used to seed initial cluster centers, and centroids are iteratively updated using similarity measures to ensure that structurally connected patches are grouped together. An adaptive threshold based on density variation and inter-cluster distance is used to combine comparable clusters and separate heterogeneous clusters, allowing the number of clusters to be determined automatically. The method converges when centroid displacement is less than a preset tolerance, assuring cluster stability.

PCA Representation of Image Patches

Consider the noisy image as:

$$I(x, y)$$

The image is separated into overlapping patches of size:

$$n \times n$$

These are reshaped into column vectors and placed into a matrix as shown in Equation (10):

$$x = [x_1, x_2, x_3, \ldots, x_m] \tag{10}$$

Where: x_i is the vectorized picture patch, represented by m, while m is the total number of patches. PCA is used on this matrix to generate a set of orthogonal basis vectors that represent the image structure's major components.

Singular Value Decomposition (SVD)

The piece of tissue matrix X is decomposed using Singular Value Decomposition as in Equation (11):

$$x = U \sum V^T \tag{11}$$

Where $X \in \mathbb{R}^{m\times n}$: Matrix generated by stacking image patches; $U \in \mathbb{R}^{m\times m}$: Left singular vector matrix; $\sum \in \mathbb{R}^{m\times n}$: Diagonal matrix containing singular values; $V^T \in \mathbb{R}^{n\times n}$: Transpose of the right singular vector matrix:

Marchenko Pastur (MP) Threshold

To discriminate between signal and noise, the Marchenko-Pastur law is employed to set a threshold for singular values. The theoretical distribution of eigenvalues of a random matrix is defined as follows in Equation (12):

$$\lambda_{\max} = \sigma_n^2 (1 + \beta)^2 \tag{12}$$

Where $\lambda_{\max}$ – The Marchenko-Pastur distribution predicts the maximum eigenvalue; σ_n^2 – Variance of the noise; $\beta = \frac{p}{n}$ – Aspect ratio of the data matrix; p – Number of variables (patch dimension); n – Number of samples (patch vectors).

The Marchenko-Pastur law states that the eigenvalues of a random noise matrix must be within a specified range. Any singular values with eigenvalues greater than $\lambda_{\max}$ are thought to contain useful signal information, whilst those below this threshold are classified as noise components.

Thus, during the PCA/SVD-based denoising process, the MP threshold is employed to distinguish between signal and noise by filtering away the singular values associated with the latter.

PCA Thresholding

After computing the singular values, thresholding is used to suppress noise components. The thresholded singular values are derived as Equation (13) for hard thresholding and Equation (14) for soft thresholding:

$$\sigma_i' = \begin{cases} \sigma_i, & if \sigma_i > T \\ 0, & if \sigma_i \leq T \end{cases} \tag{13}$$

$$\sigma_i' = \max(\sigma_i - T, 0) \tag{14}$$

Adaptive Clustering

To take advantage of structural similarity in the image, similar patches are clustered together using an adaptive clustering algorithm. Consider $x_j x_j$ two patches. A distance metric is used to determine their similarity using the Equation (15).

$$d(x_{i,} x_j) \| x_i - x_j \|_2 \tag{15}$$

Patches with similar structures are sorted into clusters, and PCA denoising is applied separately to each cluster. This increases the effectiveness of noise removal while maintaining structural features.

Methodology

As a crucial component in noise reduction, the proposed method begins by evaluating the noise intensity. The stacked patches are then subjected to adaptive clustering, which groups related patches together. MP-SVD and LMMSE progressive two-step denoising are applied to each cluster matrix. Algorithm 3 shows the algorithm of the suggested approach.

Algorithm 3

Step 1: Consider the medical images affected by Gaussian noise.
Step 2: Compute the edge detection of the noise-affected image.
Step 2.a: To compute filtering of the noise-affected image.
Step 2.b: To calculate the gradient.
Step 2.c: To create non-maximal suppressed images.
Step 2.d: To perform double thresholding.
Step 2.e: To link the edges.
Step 3: To denoise the edge-detected medical image.
Step 3. a: To estimate noise levels globally.
Step 3.b: To compute adaptive thresholding.
Step 3.c: To cluster into ‘k’ groups.
Step 3.d: To perform progressive PCA thresholding using Hard and Soft thresholding.
Step 3.e: To cluster the thresholded images into ‘k’ groups.
Step 4: To enhance the denoised image
Step 4. a: To compute membrane potential.
Step 4.b: To perform adaptive thresholding.
Step 4.c: To compute action potential.

In addition to noise removal, image enhancement is used to improve the visual quality of the reconstructed MRI pictures. While SVD-MP-based thresholding is primarily concerned with suppressing noise components in the singular value spectrum, the enhancement stage improves the contrast and visibility of anatomical structures in denoised images. This phase guarantees that critical structural elements are preserved and easily distinguished from the background. As a result, the enhancement technique improves the Contrast-To-Noise Ratio (CNR) and visual interpretability of MRI images, which is critical for medical image analysis and diagnostics.

Results and Discussion

This section discusses, verifies, and compares the findings obtained by the suggested adaptive technique in order to assess its efficacy. The experiments were carried out with brain Magnetic Resonance Imaging (MRI) images collected from the BrainWeb simulated MRI database, which is commonly utilized in medical image processing research. The grayscale images have a spatial resolution of 256×256 pixels. To test the efficiency of the proposed denoising method, Gaussian noise with various standard deviations was artificially added to the original MRI images. The noisy pictures were treated with the suggested SVD-based denoising approach and Marchenko-Pastur law thresholding. The method's performance was statistically tested using PSNR, MSE, and CNR measures.

MATLAB software is used to generate experimental results on grayscale MRI medical pictures, which are commonly employed in clinical diagnoses. MRI images are especially sensitive to noise added during acquisition, making them ideal for assessing the efficacy of denoising methods. A range of statistical metrics, including PSNR, CNR, and MSE, are assessed in order to illustrate how well the suggested method performs. The experiment begins by taking a grayscale medical image and adding Gaussian noise to it at various standard deviations, such as 10, 20, 30, 40, and 50 (Table 1).

The comparison of several denoising techniques in terms of PSNR values is shown in Table 3. The method that is suggested yields a PSNR value of 28.15 dB for a noisy image with standard deviation $\sigma = 10$. In contrast to previous approaches, the adaptive strategy yields a high PSNR value, as shown by the detailed comparison between the proposed technique and the state-of-the-art methodologies. The MSE values of the suggested method and the earlier approaches are contrasted in Table 4. At $\sigma = 10$, the suggested method achieves an MSE = 99.3507 dB value. A conclusion can be reached by comparing the approaches because the suggested approach has a lower error value than the other approaches.

DOI: 10.3844/jcssp.2026.2642.2651

Table 1: Experimental results of various Statistical parameters for MRI image

Noise Level	PSNR (dB)	MSE	CNR
10	28.1591	8.3507	0.024076
20	22.1385	397.4027	0.0248
30	19.6167	894.1561	0.024975
40	16.1179	1589.6109	0.025049
50	14.1797	2483.767	0.025089

Table 2: Comparison of various medical image denoising approaches using psnr

Denoising Method	PSNR (dB)
Kolmogorov-Smirnov distance-based MR Image denoising (Baselice et al., 2019)	28.0
Unbiased Risk Estimation based on Chi-Square (Luisier and Wolfe, 2011)	21.55
Genetic Algorithm based Local Polynomial using Intersection-Confidence Interval Filter (Dey et al., 2015)	19.59
Present Study Adaptive Algorithm	28.19

Table 3: Comparison OF various medical image denoising approaches using mse

Denoising Method	R-MSE
Median Filtering based on Multi-stage Directions (Maneesha et al., 2015)	22.75
Filtering approach based on Gaussian (Sara et al., 2019)	21.56
Linear Regression Filter using Entropy paramount (Rajalaxmi and Nirmala, 2012)	8.256
Present Study Adaptive Algorithm	8.613

Table 4: Comparison OF various medical image denoising approaches using cnr

Denoising Method	CNR
BM3D using Context (Chen et al., 2016)	2.48
curvelet-based dictionary learning based on Two-dimensions (Rabbani et al., 2017)	5.12
Image Reconstruction using Deep learning (Jensen et al., 2020)	11.58
Present Study Adaptive Algorithm	24.06

The comparison of the suggested strategy with the earlier approaches in terms of CNR value is shown in Table 5. Comparing the suggested strategy to the previous approaches, a high CNR value of 0.024076 dB is achieved. The comparison of different performance measures at different levels of σ is shown in Figures 2–4. Figure 5 shows a qualitative comparison of the noisy MRI picture and the denoised image created using the proposed adaptive progressive PCA thresholding technique. The top-left image depicts an MRI scan contaminated by Gaussian noise, with large grain-like disturbances obscuring anatomical features and reducing overall image clarity. The top-right image shows the denoised result achieved by the suggested technology, which dramatically reduces noise while keeping crucial anatomical details of brain tissues.

The experimental findings were analyzed across many noise levels (σ = 10, 20, 30, and 40) to examine the resilience of the suggested technique under various noise situations. While the results for σ = 10 illustrate the algorithm's efficacy under moderate noise, it is necessary to also analyze its behavior at greater noise levels. As the noise variance grows, the PSNR values gradually decline as the MSE increases, as expected given the higher level of corruption in the pictures. However, the suggested SVD-MP thresholding methodology outperforms conventional methods across all noise levels, suggesting that MP-based singular value thresholding effectively isolates noise components even in high-noise settings. This demonstrates the effectiveness of the proposed method for MRI image denoising.

To demonstrate the efficiency of the denoising process, the bottom row shows zoomed-in images of the respective regions. The bottom-left image depicts a noisy zoomed region in which fine anatomical characteristics are distorted due to noise interference. In contrast, the bottom-right image depicts a denoised zoomed region in which the suggested technique successfully removes noise while preserving edge information and structure.

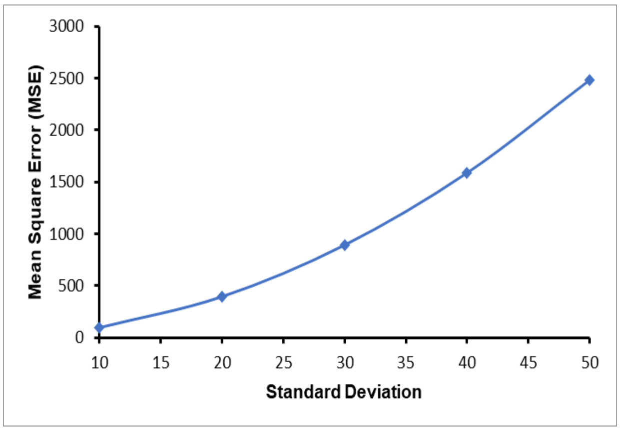

Fig. 2: Mean Square Error (MSE) MRI image at various Standard Deviations

DOI: 10.3844/jcssp.2026.2642.2651

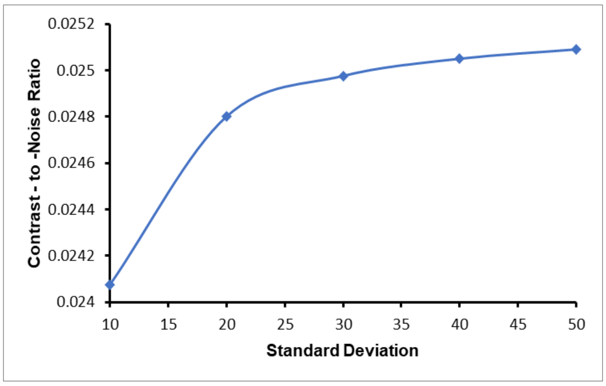

Fig. 3: Contrast - to -Noise Ratio (C-NR) MRI image at various Standard Deviations

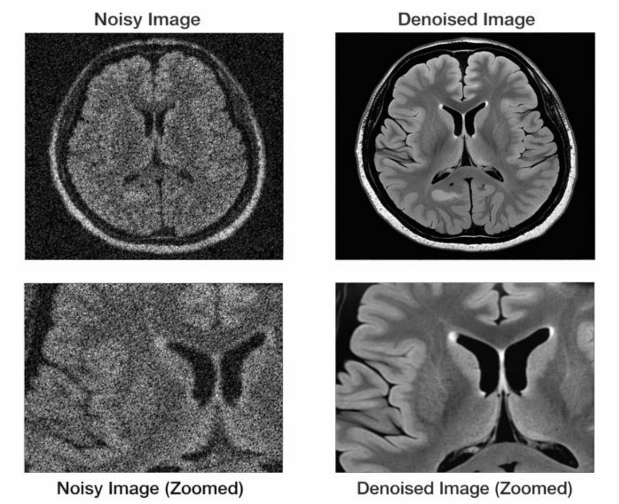

Fig. 4: The suggested method allows for a visual comparison between noisy and denoised MRI images

This visual comparison clearly shows that the suggested technique significantly lowers noise while keeping key medical image details, which are required for accurate clinical analysis and diagnosis.

The PSNR values reported in Table 2 show that the proposed adaptive denoising framework outperforms existing techniques in terms of reconstruction quality. At a noise level of σ=10, the suggested technique obtains a PSNR value of 28.19 dB, somewhat higher than the Kolmogorov-Smirnov distance-based denoising method. The improved PSNR performance indicates that the proposed method is able to effectively suppress noise while preserving important structural details in the image. This improvement can be due to the adaptive clustering technique, which groups similar image patches and allows for more effective PCA-based noise separation.

Table 3 shows the Mean Square Error (MSE) results, which reflect the success of the proposed approach. The proposed method has an MSE of 8.613, which is lower than various other filtering-based techniques. Lower MSE values suggest that the reconstructed image is more similar to the original in terms of pixel intensity. The reduction in error is mostly due to the application of progressive PCA thresholding guided by the Marchenko-Pastur law, which accurately separates signal and noise components in the single value domain.

The CNR values shown in Table 4 indicate a significant increase in contrast preservation. The suggested method has a higher CNR value than the previous alternatives, demonstrating that the algorithm can keep essential contrast information across anatomical regions. This improvement is significant for medical image analysis because increased contrast allows for improved visualization of structural boundaries.

The PSNR and CNR values achieved in this work may appear to be low due to the high amounts of Gaussian noise deliberately applied to the MRI images during the trials. PSNR values in medical image denoising tasks usually fluctuate according to noise level and image features. PSNR values in the 20-30 dB range are frequently reported in the literature for substantially distorted images, particularly when evaluating denoising performance under demanding noise settings. Similarly, CNR values vary according to the contrast between anatomical structures and background noise. Despite the challenging noise conditions used in this study, the proposed SVD-MP thresholding method consistently achieves higher PSNR and CNR values as well as lower MSE than conventional methods, indicating improved noise suppression while preserving important structural details in MRI images.

Figures 2-4 show how PSNR, MSE, and CNR vary as noise levels increase. As noise standard deviation grows from σ = 10 σ = 10 to σ = 50 σ = 50, PSNR values decline, and MSE values rise, as expected due to increased noise intensity. However, as compared to standard methodologies, the proposed strategy performs relatively consistently. This demonstrates how well the adaptive progressive PCA thresholding system handles various noise conditions.

The results in Fig. 3 show that the proposed strategy produces lower MSE values as the noise level increases. Lower MSE shows that the reconstructed images are more similar to the original MRI images, demonstrating the efficiency of the MP-based single value thresholding technique in decreasing noise components. Figure 4 shows that the suggested strategy outperforms previous approaches in terms of CNR values. Higher CNR shows more contrast between image structures and background noise, which is essential when enhancing key anatomical details in MRI scans.

Conclusion

This research described a medical image denoising method based on Singular Value Decomposition (SVD) and thresholding derived from the Marchenko-Pastur law. The MP-based cutoff offers a theoretically sound method for distinguishing noise-dominated singular values from meaningful signal components in MRI images.

Experimental evaluation of noisy brain MRI images revealed that the suggested technique effectively lowers noise while keeping essential anatomical information. The results indicate increased PSNR and CNR values, as well as lower MSE, when compared to conventional denoising techniques at various noise levels. These results show that the suggested method can produce higher-quality reconstructed images even under severe noise levels. This work's key contribution is the combination of MP-law-based adaptive singular value thresholding and SVD for medical picture denoising, which provides a systematic way for discriminating signal from noise in the singular value spectrum. The proposed method can help improve the quality of MRI images utilized in medical analysis and diagnosis.

Acknowledgment

Thank you to the publisher for their support in the publication of this research article. We are grateful for the resources and platform provided by the publisher, which have enabled us to share our findings with a wider audience. We appreciate the efforts of the editorial team in reviewing and editing our work, and we are thankful for the opportunity to contribute to the field of research through this publication.

Funding Information

The authors have not received any financial support or funding to report.

Author's Contributions

All authors have equally contributed to this manuscript.

Ethics

This article is original and contains unpublished material. The corresponding author confirms that all of the other authors have read and approved the manuscript and no ethical issues involved.

References

Ackley, D. H., Hinton, G. E., & Sejnowski, T. J. (1988). A Learning Algorithm for Boltzmann Machines. *Cognitive Science*, *9*(1), 638–650. https://doi.org/10.7551/mitpress/4943.003.0039

Agrawal, S., & Sahu, R. (2012). Wavelet based MRI image denoising using thresholding techniques. *International Journal of Science, Engineering and Technology Research (IJSETR*, *1*(3), 32–26.

Ali, H. M. (2018). MRI Medical Image Denoising by Fundamental Filters. *High-Resolution Neuroimaging - Basic Physical Principles and Clinical Applications*, 111–124. https://doi.org/10.5772/intechopen.72427

Awate, S. P., & Whitaker, R. T. (2005). Nonparametric Neighborhood Statistics for MRI Denoising. *Information Processing in Medical Imaging: 19th International Conference, IPMI 2005*, 677–688. https://doi.org/10.1007/11505730_56

Baselice, F., Ferraioli, G., Ambrosanio, M., Pascazio, V., & Schirinzi, G. (2018). Enhanced Wiener filter for ultrasound image restoration. *Computer Methods and Programs in Biomedicine*, *153*, 71–81. https://doi.org/10.1016/j.cmpb.2017.10.006

Baselice, F., Ferraioli, G., Pascazio, V., & Sorriso, A. (2019). Denoising of MR images using Kolmogorov-Smirnov distance in a non local framework. *Magnetic Resonance Imaging*, *57*, 176–193. https://doi.org/10.1016/j.mri.2018.11.022

Buades, A., Coll, B., & Morel, J.-M. (2005). A Review of Image Denoising Algorithms, with a New One. *Multiscale Modeling & Simulation*, *4*(2), 490–530. https://doi.org/10.1137/040616024

Burger, H. C., Schuler, C. J., & Harmeling, S. (2012). Image denoising: Can plain neural networks compete with BM3D? *2012 IEEE Conference on Computer Vision and Pattern Recognition*, 2392–2399. https://doi.org/10.1109/cvpr.2012.6247952

Chen, L. L., Gou, S. P., Yao, Y., Bai, J., Jiao, L., & Sheng, K. (2016). Denoising of low dose CT image with context-based BM3D. *2016 IEEE Region 10 Conference (TENCON)*. TENCON 2016 - 2016 IEEE Region 10 Conference, Singapore. https://doi.org/10.1109/tencon.2016.7848089

Chen, Q., & Wu, D. (2010). Image denoising by bounded block matching and 3D filtering. *Signal Processing*, *90*(9), 2778–2783. https://doi.org/10.1016/j.sigpro.2010.03.016

Dey, N., Ashour, A., Beagum, S., Pistola, D., Gospodinov, M., Gospodinova, E., & Tavares, J. (2015). Parameter Optimization for Local Polynomial Approximation based Intersection Confidence Interval Filter Using Genetic Algorithm: An Application for Brain MRI Image De-Noising. *Journal of Imaging*, *1*(1), 60–84. https://doi.org/10.3390/jimaging1010060

Gondara, L. (2016). Medical image denoising using convolutional denoising Autoencoders. *Data Mining Workshops (ICDMW), 2016 IEEE 16th International Conference On*, 241–246.

Hasan, M., & El-Sakka, M. R. (2018). Improved BM3D image denoising using SSIM-optimized Wiener filter. *EURASIP Journal on Image and Video Processing*, *2018*(1), 1–25. https://doi.org/10.1186/s13640-018-0264-z

He, L., & Greenshields, I. R. (2009). A Nonlocal Maximum Likelihood Estimation Method for Rician Noise Reduction in MR Images. *IEEE Transactions on Medical Imaging*, *28*(2), 165–172. https://doi.org/10.1109/tmi.2008.927338

Jain, V., & Seung, H. S. (2009). Natural image denoising with convolutional networks. *Advances in Neural Information Processing Systems*, 769–776.

Jannath, P. F., Shajun, S. isha, & DrMMohammedSathik. (2016). Noise Reduction in MRI Images using Contourlet Transform and Threshold Shrinkages Techniques". *International Journal of Computer Science and Information Technologies*, *7*(2), 723–728.

Jensen, C. T., Liu, X., Tamm, E. P., Chandler, A. G., Sun, J., Morani, A. C., Javadi, S., & Wagner-Bartak, N. A. (2020). Image Quality Assessment of Abdominal CT by Use of New Deep Learning Image Reconstruction: Initial Experience. *American Journal of Roentgenology*, *215*(1), 50–57. https://doi.org/10.2214/ajr.19.22332

Lebrun, M. (2012). An Analysis and Implementation of the BM3D Image Denoising Method. In *Image Processing On Line* (Vol. 2, pp. 175–213). https://doi.org/10.5201/ipol.2012.l-bm3d

Li, Y., Zhang, J., & Wang, M. (2017). Improved BM3D denoising method. *IET Image Processing*, *11*(12), 1197–1204. https://doi.org/10.1049/iet-ipr.2016.1110

Luisier, F., & Wolfe, P. J. (2011). Chi-square unbiased risk estimate for denoising magnitude MR images. *2011 18th IEEE International Conference on Image Processing*, 1561–1564. https://doi.org/10.1109/icip.2011.6115745

Luo, J., Wang, S., Xiao, M., Zhang, L., & Zhu, Y. (2010). Magnetic resonance image denoising using spectral data substitution. *2010 3rd International Congress on Image and Signal Processing*, 738–743. https://doi.org/10.1109/cisp.2010.5646733

Makinen, Y., Azzari, L., & Foi, A. (2019). Exact Transform-Domain Noise Variance for Collaborative Filtering of Stationary Correlated Noise. *2019 IEEE International Conference on Image Processing (ICIP)*, 185–189. https://doi.org/10.1109/icip.2019.8802964

Maneesha, M. R. M., Sulochana, C. H., & Latha, T. (2015). Medical image denoising using multistage directional median filter. *2015 International Conference on Circuits, Power and Computing Technologies [ICCPCT-2015]*, 1–6. https://doi.org/10.1109/iccpct.2015.7159261

Misra, D., Sarker, S., Dhabal, S., & Ganguly, A. (2013). Effect of using Genetic Algorithm to denoise MRI images corrupted with Rician Noise. *2013 IEEE International Conference ON Emerging Trends in Computing, Communication and Nanotechnology (ICECCN)*, 146–151. https://doi.org/10.1109/ice-ccn.2013.6528481

Pour, N., & Javanshir, A. H. (2017). A robust approach for medical image denoising using fuzzy clustering. *International Journal of Computer Science and Network Security*, *17*(6), 241–247.

Rabbani, H., Esmaeili, M., Dehnavi, A., & Hajizadeh, F. (2017). Speckle Noise Reduction in Optical Coherence Tomography Using Two-dimensional Curvelet-based Dictionary Learning. *Journal of Medical Signals & Sensors*, *7*(2), 86. https://doi.org/10.4103/2228-7477.205592

Rajalaxmi, S., & Nirmala, S. (2012). Echocardiographic image denoising and objective fidelity criteria estimation using entropy paramounted linear regression filter. *2012 International Conference on Emerging Trends in Science, Engineering and Technology (INCOSET)*, 536–541. https://doi.org/10.1109/incoset.2012.6513961

Rajan, J., Jeurissen, B., Verhoye, M., Van Audekerke, J., & Sijbers, J. (2011). Maximum likelihood estimation-based denoising of magnetic resonance images using restricted local neighborhoods. *Physics in Medicine and Biology*, *56*(16), 5221–5234. https://doi.org/10.1088/0031-9155/56/16/009

Sara, U., Akter, M., & Uddin, M. S. (2019). Image Quality Assessment through FSIM, SSIM, MSE and PSNR—A Comparative Study. *Journal of Computer and Communications*, *07*(03), 8–18. https://doi.org/10.4236/jcc.2019.73002

Sarjanoja, S., Boutellier, J., & Hannuksela, J. (2015). BM3D image denoising using heterogeneous computing platforms. *2015 Conference on Design and Architectures for Signal and Image Processing (DASIP)*, 1–8. https://doi.org/10.1109/dasip.2015.7367257

Starck, J.-L., Candes, E. J., & Donoho, D. L. (2002). The curvelet transform for image denoising. *IEEE Transactions on Image Processing*, *11*(6), 670–684. https://doi.org/10.1109/tip.2002.1014998

Sudeep, P. V., Palanisamy, P., Kesavadas, C., & Rajan, J. (2015). Nonlocal linear minimum mean square error methods for denoising MRI. *Biomedical Signal Processing and Control*, *20*, 125–134. https://doi.org/10.1016/j.bspc.2015.04.015

Xue, W., Zhang, L., Mou, X., & Bovik, A. C. (2014). Gradient Magnitude Similarity Deviation: A Highly Efficient Perceptual Image Quality Index. *IEEE Transactions on Image Processing*, *23*(2), 684–695. https://doi.org/10.1109/tip.2013.2293423

You, Y.-L., & Kaveh, M. (2000). Fourth-order partial differential equations for noise removal. *IEEE Transactions on Image Processing*, *9*(10), 1723–1730. https://doi.org/10.1109/83.869184

Zhong, H., Ma, K., & Zhou, Y. (2015). Modified BM3D algorithm for image denoising using nonlocal centralization prior. *Signal Processing*, *106*, 342–347. https://doi.org/10.1016/j.sigpro.2014.08.014